

Supplementary Information

**Assembling Laminated Films *via* Synchronous Reduction of Graphene
Oxide and Formation of Copper-Based Metal Organic Framework**

Li Li,^{†a} Ruyi Chen,^{†a} Yujiao Gong,^a Chenyang Yu,^a Zengyu Hui,^a Hai Xu,^a Xi Zhao,^a Yue Sun,^a
Wen Zhao,^a Gengzhi Sun^{*a} and Wei Huang^{ab}

^aKey Laboratory of Flexible Electronics (KLOFE) & Institute of Advanced Materials (IAM),
Nanjing Tech University (NanjingTech), 30 South Puzhu Road, Nanjing 211816, P. R. China. E-
mail: iangzsun@njtech.edu.cn

^bInstitute of Flexible Electronics (IFE), Northwestern Polytechnical University, 127 West Youyi
Road, Xi'an 710072, P. R. China.

Experimental Section

Preparation of Cu-MOF/rGO Hybrid Film: The aqueous GO dispersion was prepared according to our previous studies.¹⁻⁴ Typically, 42 mg of H₃BTC was added into 20 mL GO (2 mg mL⁻¹) mixture solution with DI water and DMF (volume ratio of 4:1) under ultrasonic dispersion for 10 min. Then the precursor was transferred to a petri dish. A piece of well-cleaned Cu foil was immersed into the above dispersion for 12 h at ambient temperature to synchronously reduce GO and form Cu-MOF on the surface of Cu foil. The obtained gel film was washed with ethanol to remove residual solvent and organic ligand, then immersed in deionized water for 20 min to remove the physisorbed GO nanosheets. Once dried at 60 °C, the hybrid film was peeled off from Cu foil.

Preparation of Bare rGO Film and Bulk Cu-MOF: Similar to the preparation of Cu-MOF/rGO, the bare rGO film was obtained by immersing Cu foil in GO aqueous solution without the addition of H₃BTC. Bulk Cu-MOF was synthesized by a hydrothermal method for control experiment. Typical, 3.6 mmol Cu(NO₃)₂ • 3H₂O were dissolved in 15 mL deionized water and mixed with 2.0 mmol of trimesic acid dissolved in 15 mL ethanol. The solution was filled in a 50 mL Teflon lined stainless steel autoclave, then sealed and kept at 120 °C for 12 h, followed by washing the obtained samples with DI water and dried at 60 °C for 6 h.

Fabrication of Cu-MOF/rGO Hybrid Film electrode: The Cu-MOF/rGO hybrid film was cut into strips with certain dimensions and fixed on a polyethylene terephthalate (PET) substrate. A copper wire (0.2 mm in diameter) was connected to the end of the films with the aid of silver paste which was insulated by a silicon rubber. The schematic of the electrode is shown in Figure S4.

Characterization: The morphology and microstructure of rGO film and Cu-MOF/rGO hybrid film were characterized using field-emission SEM (JEOL JSM7800F) and TEM (JEOL 1400PLUS). The electrical properties of bare rGO film and Cu-MOF/rGO hybrid film were characterized using Keithley 2400. Briefly, Cu-MOF/rGO film was cut into strips with length, width and thickness of l , w and h , respectively. Once the resistance (R) of the film was measured, the conductivity can be calculated according to the following equation:

$$\sigma = \frac{l}{R \cdot w \cdot h} \quad (\text{S cm}^{-1})$$

The mechanical strength of rGO film and Cu-MOF/rGO hybrid film were characterized using a universal testing instrument (HY-0350). X-ray diffraction (XRD) was taken with Smartlab (3 kW) powder X-ray diffractometer. Raman spectroscopy measurements were performed on a micro-Raman system (WITEC, Alpha 300M+) with excitation wave length of 633 nm. Nitrogen sorption measurements were

conducted with automatic volumetric adsorption equipment (Tristar II 3020) at 77 K. Before the nitrogen adsorption and desorption measurements, the samples were dried overnight at 200 °C under vacuum. The electrochemical characterizations were obtained by a CHI 660E electrochemical workstation. The electrode was tested in a three-electrode system with 1 M KOH aqueous solution as electrolyte. Pt plate and Ag/AgCl (saturated KCl) were used as counter and reference electrode, respectively.

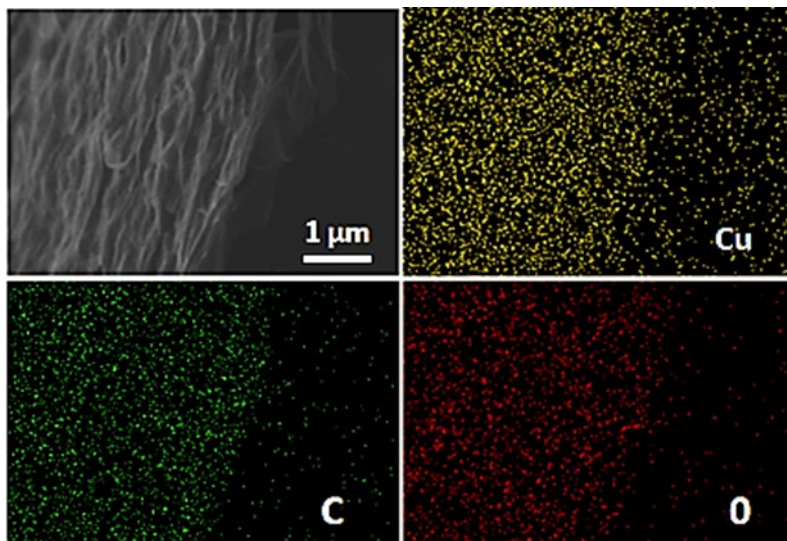


Figure S1. EDS mapping of Cu-MOF/rGO hybrid film.

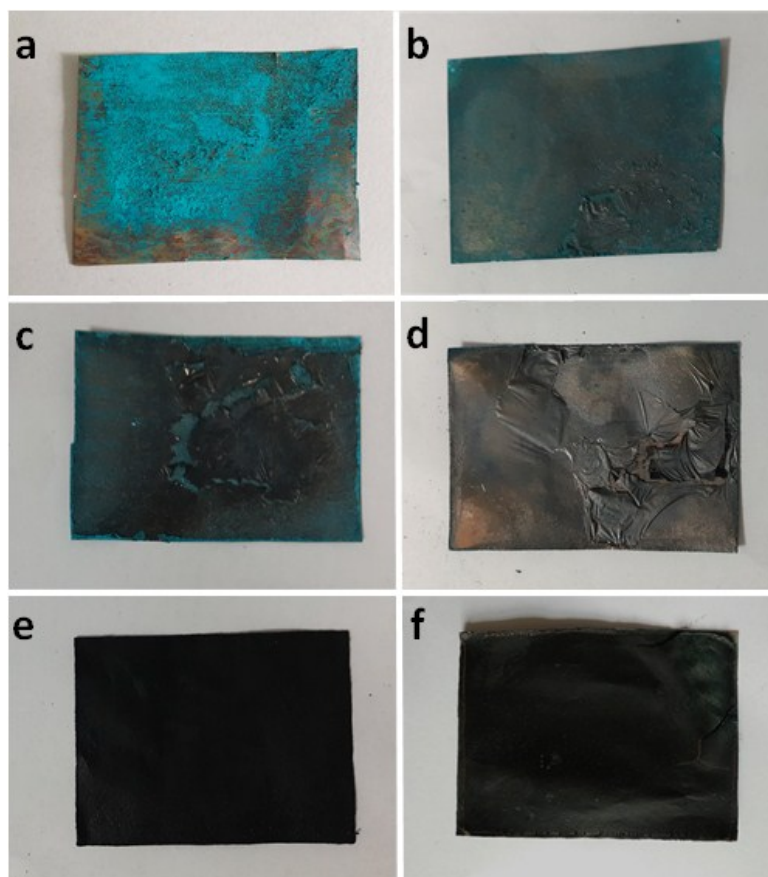


Figure S2. The growth of Cu-MOF/rGO hybrid film on the surface of copper foil with different $V_{\text{H}_2\text{O}}/V_{\text{DMF}}$ ratios. The ratio of $V_{\text{H}_2\text{O}}/V_{\text{DMF}}$ is (a) pure DMF, (b) 0.5:1, (c) 1:1, (d) 2:1, (e) 4:1, (f) pure H_2O .

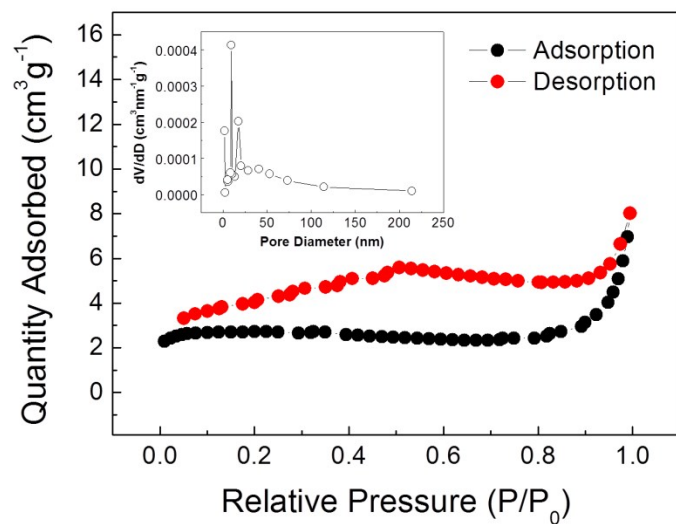


Figure S3. N₂ sorption isotherms of bare rGO film. The inset shows the pore-size distributions.

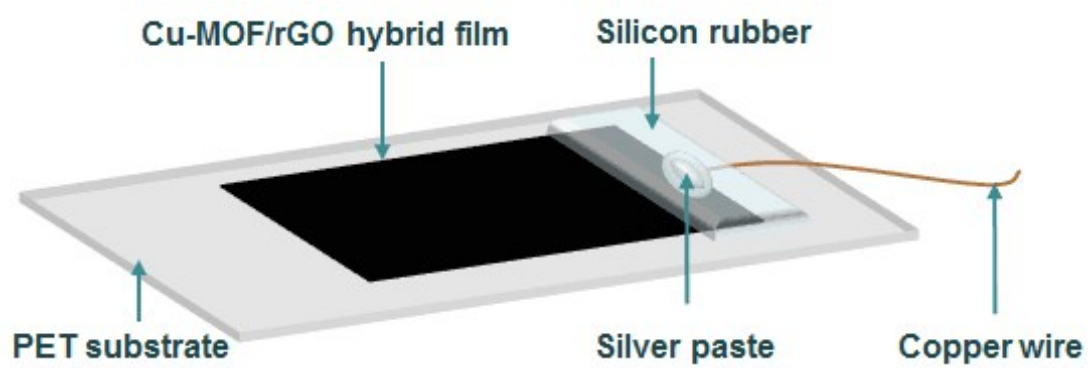


Figure S4. The schematic structure of the thin film electrode.

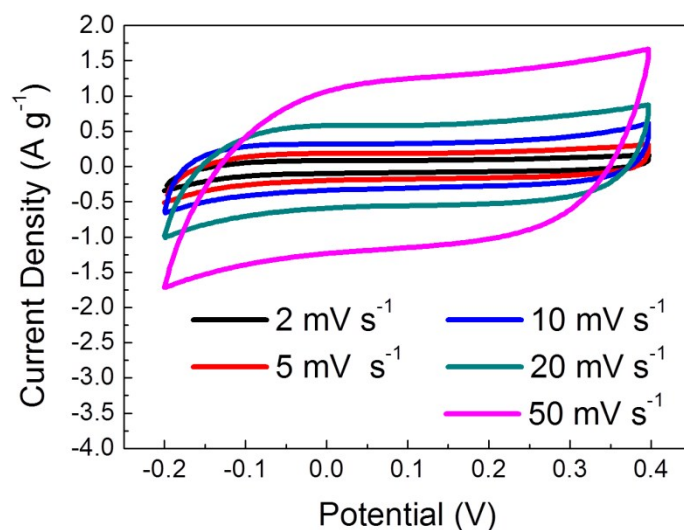


Figure S5. CV curves of bare rGO film at different scan rates.

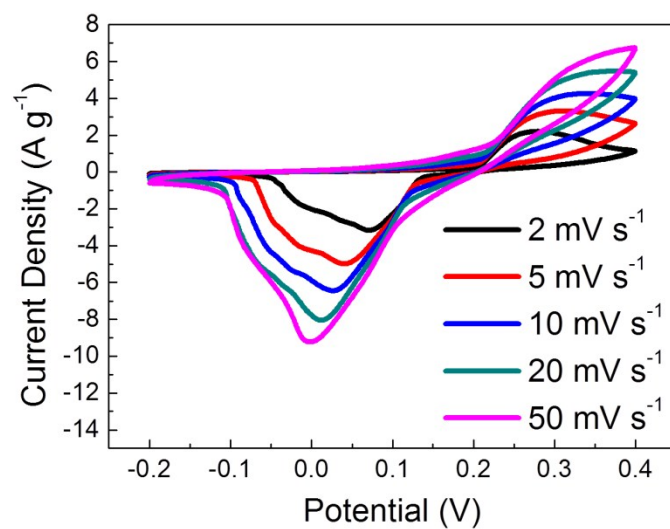


Figure S6. CV curves of Cu-MOF/rGO hybrid film at different scan rates.

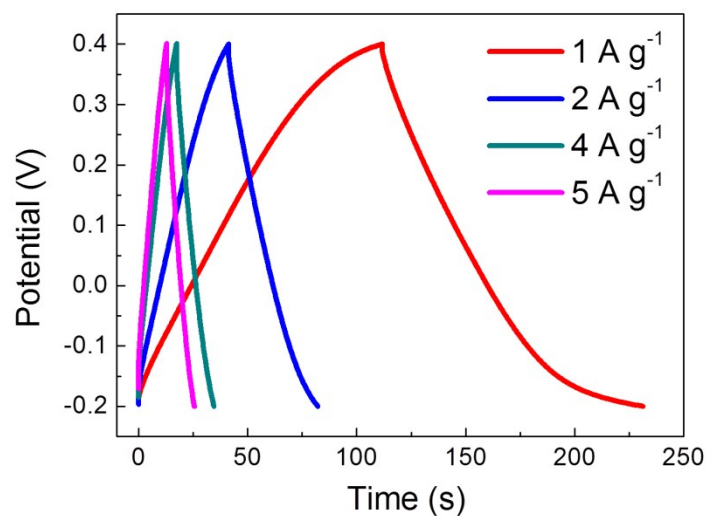


Figure S7. The galvanostatic charge-discharge curves of bare rGO film under different current densities.

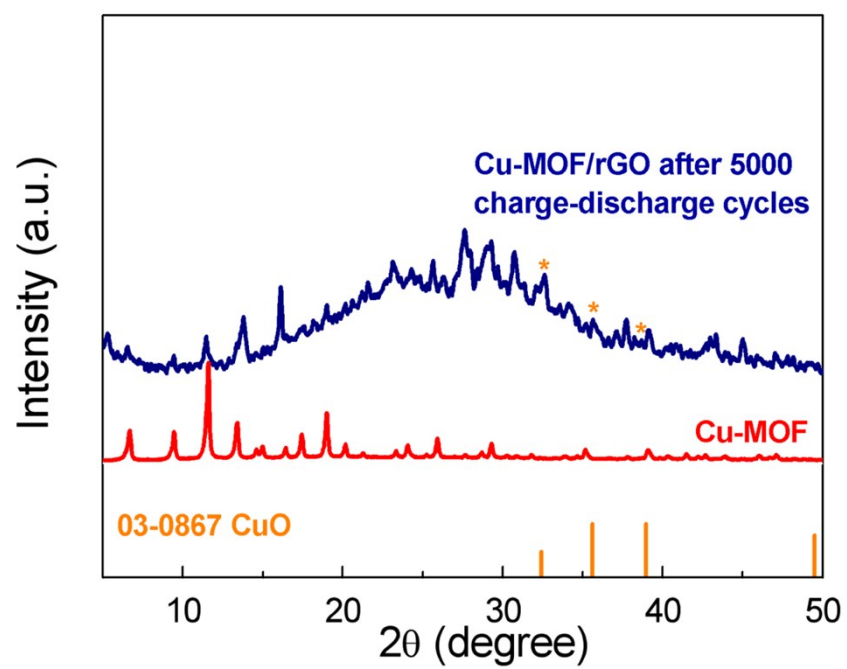


Figure S8. XRD pattern of Cu-MOF/rGO hybrid film after 5000 charge-discharge cycles.

Table S1. Performance comparison of MOF-based supercapacitor electrodes.

MOFs	Capacity	Cycling performance	References
Cu-MOF/rGO	1871 F g ⁻¹ at 0.5 A g ⁻¹	89% retained after 5000 cycles	This Work
PANI-ZIF-67-CC	371 F g ⁻¹ at 10 mV s ⁻¹	80% retained after 2000 cycles	5
Ni-HAB MOF	427 F g ⁻¹ at 0.2 mV s ⁻¹	90% retained after 12000 cycles	6
Cu-CAT MOF	202 F g ⁻¹ at 0.5 A g ⁻¹	85% retained after 2000 cycles	7
Ni-MOF	1127 F g ⁻¹ at 0.5 A g ⁻¹	90% retained after 5000 cycles	8
Ni-MOF/CNT	1765 F g ⁻¹ at 0.5 A g ⁻¹	-	9
Co-BPDC MOF	179.2 F g ⁻¹ at 10 mV s ⁻¹	87.4 retained after 1000 cycles	10
MOF-1@GO-3%	590 F g ⁻¹ at 1 A g ⁻¹	80% retained after 2000 cycles	11
[Cu ₂ Cl(OH)(L) ₂] ·(CH ₃ OH) ₄	1148 F g ⁻¹ at 0.5 A g ⁻¹	90% retained after 2000 cycles	12
Cu-MOF/rGO/GCE	685 F g ⁻¹ at 1.6 A g ⁻¹	91% retained after 1000 cycles	13

References

- 1 L. Hua, P. Shi, L. Li, C. Yu, R. Chen, Y. Gong, Z. Du, J. Y. Zhou, H. Zhang, X. Tang, G. Sun and W. Huang, *ACS Appl. Mater. Interfaces*, 2017, **9**, 37022–37030.
- 2 G. Sun, J. An, C. K. Chua, H. Pang, J. Zhang and P. Chen, *Electrochem. Commun.*, 2015, **51**, 33-36.
- 3 G. Sun, X. Zhang, R. Lin, J. Yang, H. Zhang and P. Chen, *Angew. Chem. Int. Ed.*, 2015, **127**, 4734-4739.
- 4 G. Sun, L. Zheng, Z. Zhan, J. Zhou, X. Liu and L. Li, *Carbon*, 2014, **68**, 748-754.
- 5 L. Wang, X. Feng, L. Ren, Q. Piao, J. Zhong, Y. Wang, H. Li, Y. Chen and B. Wang, *J. Am. Chem. Soc.*, 2015, **137**, 4920-4923.
- 6 D. Feng, T. Lei, M. R. Lukatskaya, J. Park, Z. Huang, M. Lee, L. Shaw, S. Chen, A. A. Yakovenko and A. Kulkarni, *Nat. Energy* 2018, **3**, 30-36.
- 7 W. H. Li, K. Ding, H. R. Tian, M. S. Yao, B. Nath, W. H. Deng, Y. Wang and G. Xu, *Adv. Funct. Mater.*, 2017, **27**, 1702067.
- 8 J. Yang, P. Xiong, C. Zheng, H. Qiu and M. Wei, *J. Mater. Chem. A*, 2014, **2**, 16640-16644.
- 9 P. Wen, P. Gong, J. Sun, J. Wang and S. Yang, *J. Mater. Chem. A*, 2015, **3**, 13874-13883.
- 10 D. Y. Lee, D. V. Shinde, E. K. Kim, W. Lee, I. W. Oh, N. K. Shrestha, J. K. Lee and S. H. Han, *Micropor. Mesopor. Mat.*, 2013, **171**, 53-57.
- 11 X. Y. Hou, X. L. Yan, X. Wang, S. n. Li, Y. Jiang, M. Hu and Q. G. Zhai, *Cryst. Growth Des.*, 2018, **18**, 6035-6045.
- 12 X. Xiong, L. Zhou, W. Cao, J. Liang, Y. Wang, S. Hu, F. Yu and B. Li,

CrystEngComm, 2017, **19**, 7177-7184.

13 M. Saraf, R. Rajak and S. M. Mobin, *J. Mater. Chem. A*, 2016, **4**, 16432-16445.